

SNR Degradation in Square-Wave Subcarrier Downconversion

Y. Feria and J. Statman
Communications Systems Research Section

This article presents a study of signal-to-noise ratio (SNR) degradation in the process of square-wave subcarrier downconversion. The study shows three factors that contribute to the SNR degradation: the cutoff of the higher frequency components in the data, the approximation of a square wave with a finite number of harmonics, and nonideal filtering. Both analytical and simulation results are presented.

I. Introduction

A square-wave subcarrier can be downconverted by using a method such as the one presented in [1]. The downconversion procedure is illustrated in Fig. 1. However, the study in [1] was done under the following assumptions: (1) the filters are ideal, (2) the data signal is band limited, and (3) the power in the higher harmonics of the square wave is negligible. These assumptions are not practical. The relaxation of these conditions will quantitatively change the output results. A measurement of this change is the signal-to-noise ratio (SNR) degradation. This article presents a study of the SNR degradation in the square-wave subcarrier downconversion using realizable filters. A pseudorandom sequence, which modulates a square-wave subcarrier approximated by the first, third, and fifth harmonics, is used as the input data. The definition of SNR degradation used here is

$$\text{SNR degradation (dB)} = \text{SNR}_{\text{ideal}} - \text{SNR}_{\text{real}}$$

where $\text{SNR}_{\text{ideal}}$ and SNR_{real} are the signal-to-noise ratios in decibels at the output of the downconverter using ideal and realizable filters, respectively.

Two types of realizable filters will be considered here: the infinite-duration impulse response (IIR) filters and the finite-duration impulse response (FIR) filters. The IIR filters are easy to implement but do not provide linear phase. The output suffers distortion due to different group delays for different frequency components. The FIR filters, on the other hand, have linear phase but need a high filter tap number, thus a long processing time.

Since the noise is additive and the downconversion system is linear, the noise and the signal can be studied separately. Then the total SNR degradation can be obtained:

$$\begin{aligned} \text{total SNR degradation (dB)} = & \text{signal power loss (dB)} \\ & + \text{noise power gain (dB)} \end{aligned}$$

II. Noise Power Change

Unlike ideal filters, a realizable bandpass filter does not have a sharp frequency cutoff; therefore, some of the noise in the stop band may be passed. On the other hand, a

realizable filter does not have a flat magnitude in the pass band; so, some of the noise in this region will be weakened, assuming unity filter gain at the center frequency. Hence, the output noise power may change as compared to the ideal case. This change can be measured as the noise power gain in decibels, defined as follows:

$$\text{noise power gain} = 10 \log \frac{\text{noise power using real filter}}{\text{noise power using ideal filter}}$$

When the value of the noise power gain is negative, the implication is that the noise power is decreased, as compared with the ideal case.

The noise power after filtering can be computed as follows: Assuming additive white noise with a power spectral density of $S(\omega) = N_0/2$, the noise power theoretically becomes [2]

$$\text{noise power} = \frac{N_0}{2} \frac{1}{2\pi} \int_{-\pi}^{\pi} |H(e^{j\omega})|^2 d\omega \quad (1)$$

where $H(e^{j\omega})$ is the filter transfer function. In the down-conversion process, both bandpass and lowpass filters are involved, and each of them will be analyzed separately in the following subsections.

A. Effect of Bandpass Filtering

For an ideal bandpass filter (BPF), the noise power becomes

$$\text{noise power using ideal filter} = |H|^2 f_B / (f_s/2)$$

where $|H| = 1$ is the filter magnitude, f_B is the BPF bandwidth, and f_s is the sample rate.

For the IIR filter, the Butterworth bandpass filters are chosen as an example since they have a maximally flat magnitude. The integral can be computed through an equivalent lowpass filter (LPF) transfer function [3, p. 421]:

$$\int_{-\pi}^{\pi} |H(e^{j\omega})|^2 d\omega = \int_{-\pi}^{\pi} \frac{1}{1 + \left[\frac{\tan(\omega/2)}{\tan(\omega_c/2)} \right]^{2N}} d\omega$$

where ω_c is the cutoff angular frequency that takes values from 0 to π , π corresponds to half of the sample frequency, and N is the filter order.

If the FIR bandpass filters are used, the integrals can be evaluated by using Parseval's theorem [3, p. 187]:

$$\sum_{n=-\infty}^{\infty} |h[n]|^2 = \frac{1}{2\pi} \int_{-\pi}^{\pi} |H(e^{j\omega})|^2 d\omega$$

Since $h[n]$ has a finite duration, the sum is over a finite number of terms.

The IIR filters are obtained by converting the analog Butterworth filters, using bilinear transformation with frequency prewarping. The cutoff frequency is the half-power or 3-dB cutoff frequency. The FIR filters are designed using the classical method of windowed linear-phase FIR filter design. A Hamming window is used in this case.

By varying the IIR filter order and the cutoff frequency, a series of integrals is numerically evaluated, and the noise power gain in decibels is computed at a sample rate of 260 kHz as shown in Table 1. For comparison, a simulation of the bandpass filtering process is realized with white Gaussian noise as the input. For the output variance to be less than 0.02 dB, the simulation was run with 5×10^6 samples (see Appendix A) at a sample rate of 260 kHz. The results are also shown in Table 1.

A similar series of results is obtained for the FIR filters. The designed FIR filters, however, may not have the half-power cutoff frequency matching the goal cutoff frequency. For a fair comparison, the half-power cutoff frequencies are obtained. The results are shown in Table 2.

Taking the difference of the analytical and simulation results in Tables 1 and 2, it is found that the largest difference in decibels is about 0.03 dB.

B. Effect of Down-Mixing

Unlike the bandpass filtering, whose effect on the noise power can be computed analytically, the effect of the down-mixing process on the noise power can be studied more easily through simulation since the noise is no longer white. The BPF's are assumed to have the same order and bandwidth at different center frequencies. It is assumed that the lowpass filter has the same order as the bandpass filters and that its bandwidth is three times that of the BPF. The filter gain is assumed to be 1 at the center frequency. The simulation was done with 5×10^6 samples at a sample rate of 260 kHz for filter bandwidths less than 5 kHz, and at 270 kHz otherwise. The results are shown in Table 3.

III. Signal Power Change

There are three factors that cause the degradation in signal power: the cutoff of the data bandwidth, the finite number of harmonics considered, and the nonideal filtering. These are next discussed individually.

A. Data Bandwidth Cutoff

The bandwidth of the BPF should be greater than or equal to the data bandwidth if the data are band limited. However, this may not be satisfied in practice.

In the simulation, the signal consists of a square-wave subcarrier modulated by a 1-kHz pseudorandom sequence as data. A pseudorandom-noise (PN) shift register generator of length 10 associated with $\{3, 10\}$ is used to generate the data [4, p. 342]. The power spectral density of the PN sequence is [4, p. 380]

$$P_{PN}(f) = -\frac{1}{N}\delta(f) + \frac{N+1}{N^2}\text{sinc}^2(\pi f T_c) \sum_{m=-\infty}^{\infty} \delta\left(f + \frac{m}{NT_c}\right)$$

where N is the sequence length, and T_c is the chip time. Clearly, a PN sequence is not band limited. Hence, when the BPF's are applied to a data modulated square-wave subcarrier, some of the signal power carried by the higher frequency components is filtered out, which leads to a signal power degradation. In general, the wider the filter bandwidth is, the lower the signal power degradation is. This relationship is shown in Fig. 2. However, there are upper limits on the filter bandwidth so that the undesirable harmonic terms can easily be separated from the desired ones [1]. For instance, in the simulation, the restriction is $22.5 \text{ kHz} - f_B/2 \geq 3f_B$, which implies that the filter bandwidth, f_B , should not exceed 6.43 kHz because aliasing may occur beyond this point. An alternative downconversion procedure (see Appendix B) may be used where no upper limit on the filter bandwidth will apply. However, the goal is to keep the bandwidth narrow for a low sample rate.

B. Finite Number of Harmonics Considered

Another factor that causes the signal power degradation is that only the first, third, and fifth harmonics are downconverted. The first three harmonics of a square-wave subcarrier carries only 93.3 percent of the total power of the square wave. So, there is about a 0.3-dB signal power

degradation in neglecting the higher order harmonics. Table 4 shows the relationship between the power loss and the harmonic number up to which the downconversion is carried out.

C. Nonideal Filtering

Finally, the signal degradation, due to the nonideal filtering, is analyzed through simulation. To separate the nonideal filtering effect from the other two factors, the input signal is considered to have the first three harmonics only:

$$\text{subcarrier} = \frac{4}{\pi} \left[\sin(2\pi ft) + \frac{1}{3} \sin(2\pi \times 3ft) + \frac{1}{5} \sin(2\pi \times 5ft) \right]$$

where $f = 22.5 \text{ kHz}$ for the Galileo signal. The simulation results can be subtracted from the signal power degradation due to the data-bandwidth cutoff computed in Section III.A. The results obtained directly from the simulation are shown in Table 5 and Figs. 3 and 4. These results reflect the signal power degradation due to both data-bandwidth cutoff and nonideal filtering. The signal degradation due to only nonideal filtering is shown in Table 6 and Figs. 5 and 6. This simulation was done with 5×10^6 samples at a sample rate of 260 kHz for filter bandwidths less than 5 kHz, and at 270 kHz otherwise.

Elliptic lowpass and bandpass filters have been simulated as well. The results in signal power degradation are lower than those using the same order Butterworth filters, but the output is severely distorted.

IV. SNR Degradation

Finally, the total SNR degradation can be obtained by adding the noise power gain in Table 3 to the signal power loss in Table 5. The results are shown in Table 7 and Figs. 7 and 8.

Note that the results in Table 7 exclude the effect of the consideration of a finite number of harmonics for the square wave.

V. Conclusion

This article presented an analysis on the SNR degradation in the square-wave subcarrier downconversion pro-

cess, as may be used in the Galileo S-band mission. There are three factors that affect the SNR degradation: the data-bandwidth cutoff, the approximation of a square wave with a finite number of harmonics, and nonideal

filtering. The three factors were analyzed separately, and the analytical and simulated results were presented. The distortion effects on the detection were not considered.

Acknowledgment

The authors thank Edgar Satorius for his many helpful suggestions and contributions to this work.

Table 1. Noise power gain (dB) due to IIR BPF.

Filter order	Filter bandwidth, kHz				
	2	3	4	5	6
6 (analytical)	0.1999	0.1993	0.1986	0.1977	0.1965
8 (analytical)	0.1120	0.1117	0.1114	0.1109	0.1104
10 (analytical)	0.0716	0.0714	0.0712	0.0709	0.0706
6 (simulated)	0.1760	0.1915	0.1899	0.2046	0.1957
8 (simulated)	0.1169	0.1004	0.1262	0.1108	0.1080
10 (simulated)	0.0926	0.0611	0.0785	0.1080	0.0732

Table 2. Noise power gain (dB) due to FIR BPF.

Filter order	Intended filter bandwidth, kHz				
	2	3	4	5	6
	Obtained filter bandwidth, kHz				
160	2.2820	2.5420	3.0620	3.7640	4.6740
320	1.5280	2.3340	3.3480	4.3360	5.3500
	Noise power gain, dB				
160 (analytical)	0.2447	0.2678	0.1513	0.0915	0.0336
320 (analytical)	0.1583	0.0386	0.0129	0.0155	0.0266
160 (simulated)	0.2304	0.2646	0.1303	0.0998	0.0123
320 (simulated)	0.1560	0.0739	-0.0012	-0.0032	0.0198

Table 3. Noise power gain (dB) in downconversion.

Filter order	Filter bandwidth, kHz				
	2	3	4	5	6
IIR 6	-0.0646	-0.0801	-0.0801	-0.0801	-0.0795
IIR 8	-0.0752	-0.0882	-0.0827	-0.0960	-0.0711
IIR 10	-0.0743	-0.0943	-0.0748	-0.0736	-0.0998
FIR 160	-	-0.1429	-0.1610	-0.1422	-0.1501
FIR 320	-0.1328	-0.1009	-0.1210	-0.0451	-0.0664

Table 4. Signal power loss due to finite number of harmonics.

Harmonic number	1st	3rd	5th	7th	9th
Power loss, dB	0.9121	0.4545	0.3009	0.2246	0.1719
Harmonic number	11th	13th	15th	17th	19th
Power Loss, dB	0.1489	0.1274	0.1113	0.0988	0.0888

Table 5. Signal power loss (dB) from simulation.

Filter order	Filter bandwidth, kHz				
	2	3	4	5	6
IIR 6	0.5069	0.3554	0.2639	0.2105	0.1780
IIR 8	0.4816	0.3422	0.2484	0.1999	0.1661
IIR 10	0.4708	0.3351	0.2403	0.1946	0.1604
FIR 160	-	0.5851	0.4807	0.3857	0.2772
FIR 320	1.0134	0.5556	0.3120	0.2253	0.1813

Table 6. Signal power degraded (dB) due to nonideal filtering.

Filter order	Filter bandwidth, kHz				
	2	3	4	5	6
IIR 6	0.0517	0.0413	0.0393	0.0284	0.0295
IIR 8	0.0318	0.0281	0.0238	0.0178	0.0176
IIR 10	0.0210	0.0210	0.0157	0.0125	0.0119
FIR 160	-	0.1653	0.1643	0.1366	0.0462
FIR 320	0.4936	0.1134	0.0464	0.0063	-0.0136

Table 7. Total SNR degradation (dB) in downconversion.

Filter order	Filter bandwidth, kHz				
	2	3	4	5	6
IIR 6	0.4413	0.2753	0.1837	0.1304	0.0985
IIR 8	0.4064	0.2541	0.1657	0.1039	0.0950
IIR 10	0.3964	0.2407	0.1655	0.1210	0.0606
FIR 160	-	0.4422	0.3197	0.2435	0.1271
FIR 320	0.8806	0.4547	0.1910	0.1802	0.1149

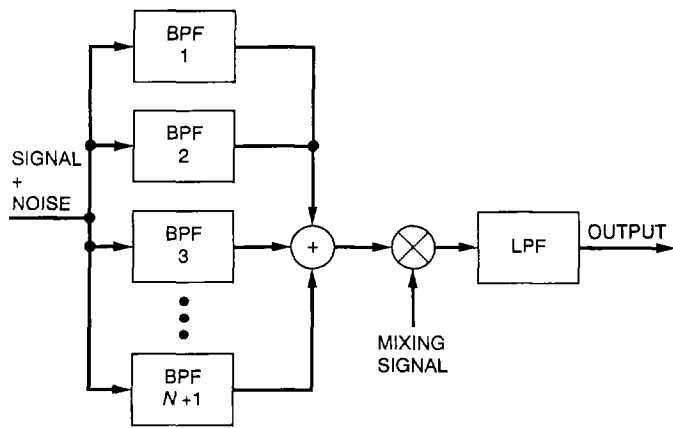


Fig. 1. Square-wave subcarrier down-conversion.

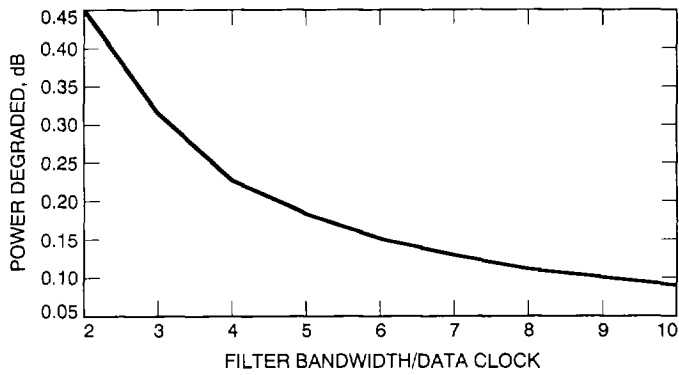


Fig. 2. Signal power degradation due to the PN bandwidth cutoff.

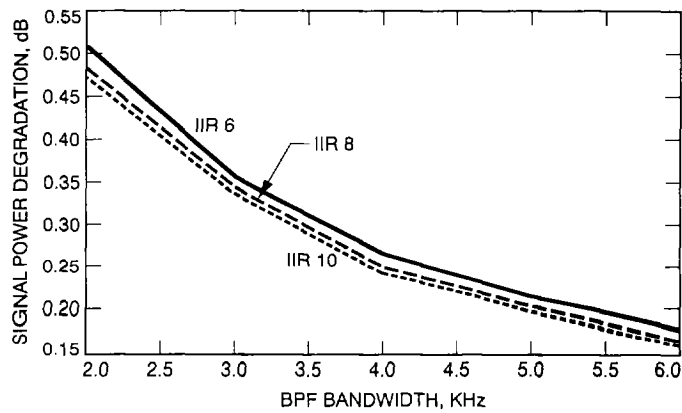


Fig. 3. Signal power degradation in downconversion using IIR filters.

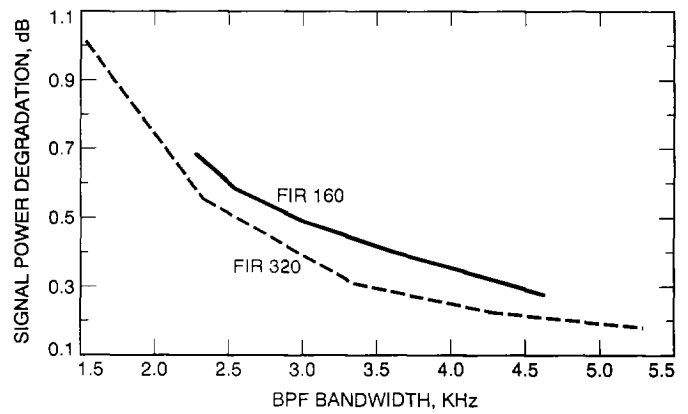


Fig. 4. Signal power degradation in downconversion using FIR filters.

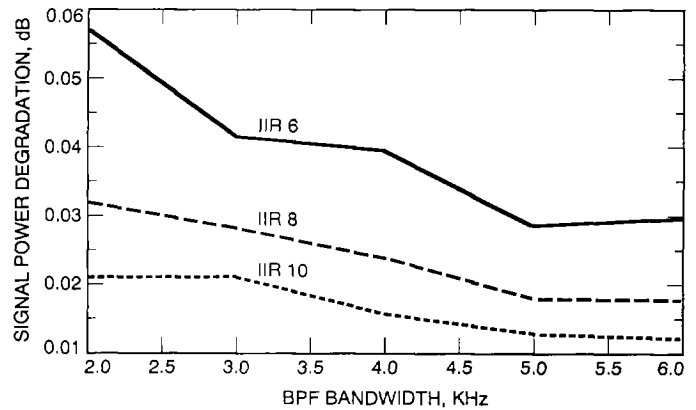


Fig. 5. Signal power degradation due to IIR filtering.

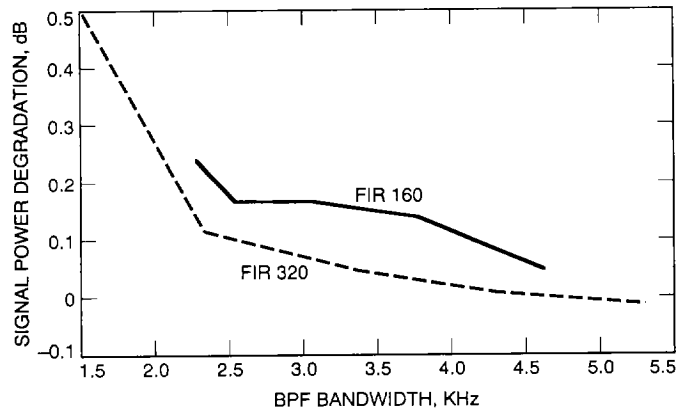


Fig. 6. Signal power degradation due to nonideal FIR filtering.

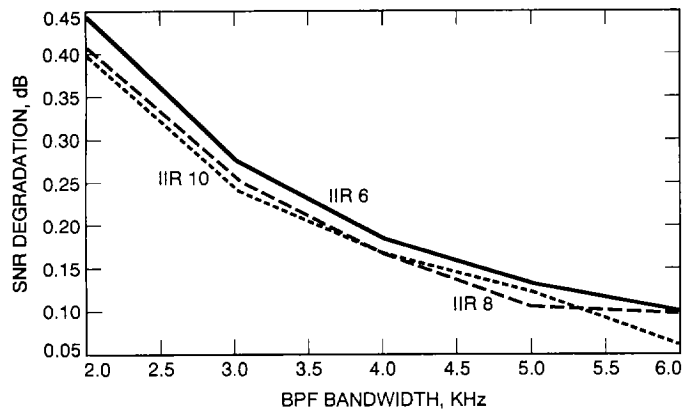


Fig. 7. SNR degradation in downconversion using IIR filters.

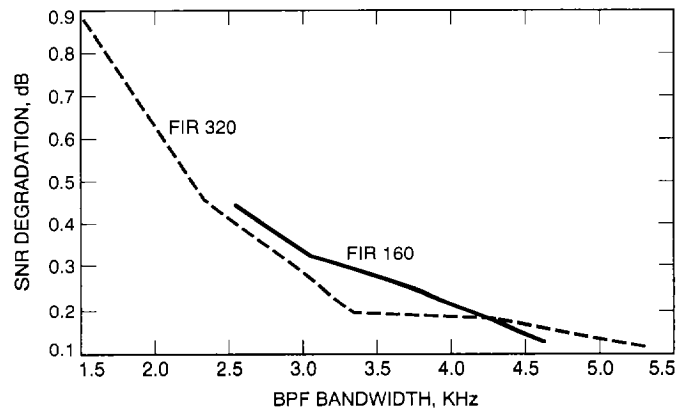


Fig. 8. SNR degradation in downconversion using FIR filters.

Appendix A

Number of Samples Needed in the Simulation

For N independent samples, x_i , of a random variable, x , the variance can be estimated by using an asymptotically unbiased and consistent estimate [5], namely,

$$\hat{\sigma}^2 = \frac{1}{N} \sum_{i=1}^N (x_i - \hat{M})^2 \quad (\text{A-1})$$

where \hat{M} is the mean estimate

$$\hat{M} = \frac{1}{N} \sum_{i=1}^N x_i$$

The mean of the variance estimate is

$$E\{\hat{\sigma}^2\} = \frac{N-1}{N} \sigma^2$$

where σ^2 is the true variance, and the variance of the estimate is

$$\text{Var}\{\hat{\sigma}^2\} = \frac{1}{N} (E\{x^4\} - E^2\{x^2\}) \quad (\text{A-2})$$

Assuming that the noise has a normal distribution, $E\{x^4\} = 3E^2\{x^2\}$ [6]. Substituting the last expression in Eq. (A-2),

$$\text{Var}\{\hat{\sigma}^2\} = \frac{2}{N} (\sigma^2)^2 \quad (\text{A-3})$$

or

$$\text{standard deviation}\{\hat{\sigma}^2\} = \sqrt{\frac{2}{N}} \sigma^2$$

where N is the number of independent samples. In this case, at the BPF output, the number of independent samples reduces to approximately $N_{in} f_B / (f_s / 2)$, with N_{in} being the number of independent samples at the input, f_B being the BPF bandwidth, and f_s being the sample rate. When $N_{in} = 5 \times 10^6$ and $f_s = 260$ kHz, the deviations (in decibels) of the estimated variance, $\hat{\sigma}^2$, from the true variance, σ^2 , in terms of f_B are shown in Table A-1.

Table A-1. Deviation of the estimated variance (dB) at output of BPF.

BPF bandwidth (kHz)	2	3	4	5	6
10 log ($\hat{\sigma}^2/\sigma^2$)	0.0210	0.0180	0.0156	0.0140	0.0128

Appendix B

An Alternative Downconversion Procedure

An alternative procedure for the square-wave subcarrier downconversion is shown in Fig. B-1. This procedure differs from the one shown in Fig. 1 in the following ways: The undesirable terms will reside in a farther region in the frequency domain. For instance, assuming that the subcarrier frequency is smaller than the mixing signal frequency, $f_s < f_m$, then the lowest frequency of the undesirable terms in the procedure of Fig. 1 is

$$7f_s - 5f_m = 2f_s + 5(f_s - f_m)$$

whereas in the alternative procedure, this frequency is

$$f_s + f_m = 2f_s + (f_m - f_s)$$

The second term of the last two expressions are negative and positive, respectively. This fact makes the lowest frequency of the undesirable terms in the second case much larger than the first case, which is desired since this may lead to lesser interference from the undesirable terms when nonideal filters are realized. From the hardware perspective, this procedure may need four multipliers and three adders versus six adders and one multiplier in the procedure shown in Fig. 1.

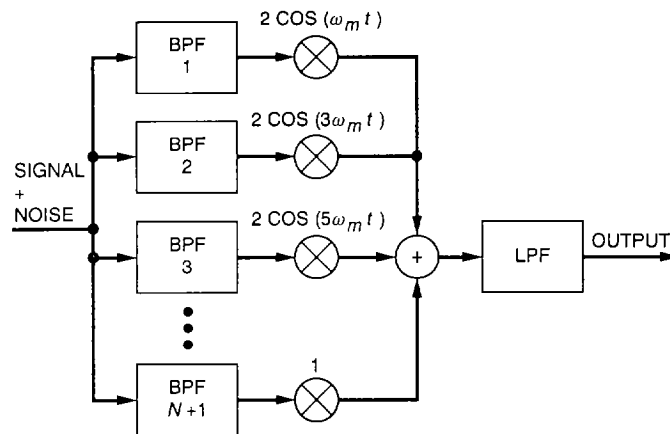


Fig. B-1. Alternative procedure for square-wave subcarrier downconversion.

References

- [1] Y. Feraia and J. Statman, "Bandwidth Compression of Noisy Signal With Square-Wave Subcarrier," *TDA Progress Report 42-109*, vol. January–March 1992, Jet Propulsion Laboratory, Pasadena, California, pp. 170–178, May 15, 1992.
- [2] A. B. Carlson, *Communication Systems—An Introduction to Signals and Noise in Electrical Communication*, 3rd ed., New York: McGraw-Hill, pp. 174–176, 1986.
- [3] A. V. Oppenheim and R. W. Schaffer, *Discrete-Time Signal Processing*, Englewood Cliffs, New Jersey: Prentice Hall, 1989.
- [4] J. K. Holmes, *Coherent Spread Spectrum Systems*, Malabar, Florida: Robert E. Krieger Publishing Company, 1990.
- [5] R. L. Fante, *Signal Analysis and Estimation*, New York: John Wiley and Sons, pp. 353–354, 1988.
- [6] A. Papoulis, *Probability, Random Variables, and Stochastic Processes*, New York: McGraw-Hill, p. 148, 1965.